

Oxygen and water vapour transport in cement–silica fume pastes

Cabrera, J.G. and Claisse, P.A.

Author post-print (accepted) deposited in CURVE June 2010

Original citation & hyperlink:

Cabrera, J.G. and Claisse, P.A. (1999) Oxygen and water vapour transport in cement–silica fume pastes. *Construction and Building Materials*, volume 13 (7): 405-414

[http://dx.doi.org/10.1016/S0950-0618\(99\)00039-2](http://dx.doi.org/10.1016/S0950-0618(99)00039-2)

Copyright © and Moral Rights are retained by the author(s) and/ or other copyright owners. A copy can be downloaded for personal non-commercial research or study, without prior permission or charge. This item cannot be reproduced or quoted extensively from without first obtaining permission in writing from the copyright holder(s). The content must not be changed in any way or sold commercially in any format or medium without the formal permission of the copyright holders.

This document is the author's post-print version of the journal article, incorporating any revisions agreed during the peer-review process. Some differences between the published version and this version may remain and you are advised to consult the published version if you wish to cite from it.

CURVE is the Institutional Repository for Coventry University

<http://curve.coventry.ac.uk/open>

OXYGEN AND WATER VAPOUR TRANSPORT IN CEMENT-SILICA FUME PASTES

by

J G CABRERA* AND P A CLAISSE**

* Civil Engineering Materials Unit, School of Civil Engineering, University of Leeds, Leeds, LS2 9JT, UK

** Department of the Built Environment, Coventry University, Coventry, CV1 5SB, UK

ABSTRACT

Partial replacement of cement with Silica Fume (SF) has been proposed as a method of reducing the corrosion rate of embedded reinforcing steel in concrete. Experimental work has been carried out to determine the effect of the SF on the transport rates of oxygen and water in cementitious samples.

By analysing the effect of different pressure drops across the samples it is concluded that the flow of oxygen is described by the Darcy equation, but the flow of water vapour is not. The different mechanisms of transmission cause the transmission rates for oxygen to be spread over a far greater range than those for water vapour with some of the SF samples almost impermeable to oxygen.

INTRODUCTION

In order to sustain the corrosion of reinforcing steel in concrete it is necessary that both oxygen and water are transported through the cover to the bars. Both materials must penetrate the same depth of cover in order to reach the reaction site from the external

environment. If the corrosion process is subject to control from these processes, it will therefore be limited by the material which has the slowest transport rate through concrete.

For the oxygen the situation is relatively simple because it will generally be transported as a gas. There will be some contribution from solution-diffusion in wet concretes, but this is unlikely to be significant in structures which are not submerged in water. For the water there are three possible mechanisms, some may enter the concrete as a liquid, some may enter as vapour and condense and some may be transported as vapour.

Partial cement replacement with Silica Fume (SF) has been proposed as a method of reducing the corrosion of reinforcement in concrete (1). The experiments described in this paper are intended to show the effect of this replacement on the transmission of water vapour and oxygen.

EXPERIMENTAL METHODS

Mix Designs and Curing

Two mortar mixes with OPC + SF and two with OPC were used. The mix details are shown in Table 1.

Table 1. Mix Proportions

Mix	A	B	C	D
Silica Fume/(Cement + SF)	0.20	0	0.20	0
Water/(Cement + SF)	0.30	0.30	0.46	0.46
Superplasticiser/(Cement + SF)	0.014	0.014	0.019	0.019
Fine Aggregate/(Cement + SF)	1.5	1.5	2.3	2.3

The SF was supplied by Elkem Chemicals from their works in Norway. The superplasticiser was a salt of naphthalene formaldehyde condensate supplied by FEB (UK). The fine aggregate came from North Nottinghamshire and was a natural sand with a grading in zones 2-3 to BS882 (2). The percentages given for superplasticiser were calculated from the quantities of solids which form 40% of the solution as supplied. Paste samples were made with the same proportions without the fine aggregate.

The samples were mixed in a Hobart mixer. The superplasticiser was mixed with the water and added to the sand and cement when they had already been mixed in a dry condition. Mixing continued for two minutes after a uniform consistency was observed. The highest speed of the mixer was used for the mixes with lower workability but for those with highest workability this caused them to be ejected from the mixer and a lower speed was used. The samples were cast in the appropriate moulds, kept covered in the laboratory for 24 hours and then placed in the following curing conditions.

Curing Condition 1 (CC1): 99% RH, 20°C

Curing Condition 2 (CC2): Treated with curing membrane and then stored at
70% RH, 20°C for 6 days and then in water at 6°C

Curing Condition 3 (CC3): In water at 6°C

The temperature of 6°C was chosen as being the lowest at which mixes of this type should be placed on a well managed site.

MEASUREMENT OF OXYGEN TRANSMISSION

Apparatus

The apparatus used for testing was designed by Cabrera and Lynsdale (3). The rate of flow was measured with a bubble flow meter. The apparatus is shown in Figure 1. The

seal is formed by first coating the curved surface of the sample with silicone rubber and then compressing it into a surround of synthetic rubber.

Preparation of the Samples

Mortar samples were cast as 100 mm cubes. When they were struck, 25 mm cores were cut from them and 20 mm long samples were cut from the central portion of the cores.

At the test age the samples were dried for 24 hours and at 105°C and placed in a dessicator. When they had cooled, a thin film of silicone rubber was applied to the curved surfaces and allowed to set for 24 hours before testing.

Before testing the “Curing Condition 2” samples, any remaining curing agent on the end surfaces was removed using No. 40 grit sandpaper. Penetration of this material into the pores could, however, have reduced the flow rates but inspection of the samples indicated that this would not have been significant.

Testing Procedure

The samples were tested at applied oxygen pressures of 1 and 2 atmospheres above ambient. Two samples were tested for each condition. Before testing, the samples were allowed a minimum of 30 minutes to equilibrate and to purge the air from the system and for samples with very low flow rates this was increased to several hours. Two readings were taken on each sample at each pressure and the average of these two readings was used. Different diameter bubble flow meters were used ranging from 1.7 mm for very low flows, to 10 mm for high flows.

Leakage was checked using some spare samples, these were spread with silicone rubber over the flat surfaces as well as the curved surface and checking that there was no gas flow. No flow was observed. If there had been any substantial leakage the range of the data would have been increased.

Calculation of a Coefficient

The Basis of the Method:

Lawrence (4) discusses a number of different possible coefficients of permeability. In later work Lawrence (5) uses a method based on Darcy's law. This has also been used by Bamforth (6), Nagataki and Ujike (7) and Cabrera and Lynsdale (3) and is easily derived as follows.

For one dimensional flow Darcy's law states that:

$$v = \frac{k}{e} \cdot \frac{dp}{dx} \quad (1)$$

Where:

v = velocity of the fluid

k = coefficient of permeability

e = viscosity of the fluid

x = distance from the surface of the sample

p = pressure at position x (all pressures are measured relative to vacuum)

If Q is the volume per second passing through the sample measured at the low pressure P_1 (assuming an ideal gas):

$$Q = v \cdot A \cdot \frac{P}{P_1} \quad (2)$$

Where:

A = cross sectional area of the sample

P_1 = the low pressure (i.e. the pressure on the outlet side of the sample, this is atmospheric pressure in this work)

$$\frac{Q}{A} \cdot \frac{P_1}{p} = \frac{k}{e} \cdot \frac{dp}{dx} \quad (3)$$

and:

$$\frac{dx}{dp} \cdot \frac{A \cdot k}{Q \cdot e \cdot P_1} \cdot p \quad (4)$$

integrating across the sample:

$$t = \frac{A \cdot k (P_2^2 - P_1^2)}{2Q \cdot e \cdot P_1} \quad (5)$$

Where:

P_2 = high pressure (i.e. the pressure on the input side of the sample)

t = sample thickness

Thus:

$$k = \frac{2 \cdot t \cdot Q \cdot e \cdot P_1}{A (P_2^2 - P_1^2)} \quad (6)$$

The viscosity of oxygen gas $e = 2.02 \times 10^{-5} \text{ Ns/m}^2$

$P_1 = 1 \text{ atmosphere} = 0.101 \text{ MPa}$

Relationship between readings at different pressures

The relationship between the readings at the two pressures is shown in Figure 2 which is plotted logarithmically to spread the readings. It may be seen that the data lie very accurately on the line of equality indicating that the use of Darcy's equation was justified. The average of the two readings was calculated and is plotted in Figure 3.

MEASUREMENT OF VAPOUR TRANSMISSION

Preparation of the Samples

Paste samples for measurement of water vapour transport were cast as 100 mm cubes and 25 mm diameter cores were cut from them before curing. At the test age thin discs were cut from the central portion of the cores. The thickness of each disc was measured with a micrometer. The thickness of all the discs fall in the rang of 3.5 - 4.7 mm. The discs were permitted to dry at room temperature for approximately two hours and then set in epoxy resin in holes formed in the lids of 125 cc sample bottles. The bottles were then part filled with de-ionised water and the lids put on them and sealed as shown in Figure 4. The effectiveness of the seals was checked by briefly inverting the bottles. the bottles were then placed in trays in large storage containers. Details of the environmental conditions in the containers are as follows:

All of the containers were kept at 21°C. The RH was checked periodically using an electronic probe.

The water transmission rate was measured by weighing the bottles. Two samples were tested for each of the 4 mixes, 3 curing conditions, 3 test ages and 3 containers to give a total of 216 bottles.

Blank Tests

In addition to the sets of cementitious samples, a number of blank samples (coins) were tested. No measurable weight loss occurred and this confirmed that the bottles and seals were impermeable and the only transmission path was through the samples.

ANALYSIS OF THE DATA

Initial preparation

The weights of the bottles were initially plotted against time, a typical plot showing results of 6 samples is shown in Figure 5. These plots were used to identify bottles where obvious leakage was causing a wrong result. Out of the total of 216 bottles, there were 3 of this type and the results from them were not used.

Interpretation of the data

It may be seen from Figure 4 that the initial mass loss rate is higher than the steady state. The following two processes are believed to contribute to this effect.

1. When the samples were first installed they had a relatively constant moisture content throughout. Whatever the final distribution, it was certainly not constant across the thickness. An increase in moisture content on the wet side would not affect the measured weight but a loss from the dry side would cause a loss of weight. The factors controlling the exact rate of moisture loss are complex because the rate of migration of water will depend on the local humidity gradient and the total amount to be lost from any given depth will depend on the final distribution. As a rough approximation it is, however, reasonable to assume an exponential decay, i.e. the rate of loss will be proportional to the amount remaining to be lost.
2. When the samples were installed they were not fully hydrated. Due to the presence of moisture the hydration will have continued and the hydration products will have formed in previously open pores. The factors controlling the transmission rate are again complex because the rate of hydration will depend on the availability of water. An exponential decay may be very approximately justified by assuming that the rate of hydration depends on the quantity of cement

remaining to hydrate and the rate of transmission decreases linearly with the quantity of hydration products present. Thus the rate of hydration will decay exponentially and the rate of transmission will follow it.

If the two processes are assumed to proceed at approximately the same speed they may be represented by a single term to describe the initial additional losses, i.e.

$$M_0 e^{-Kt}$$

Where, K is a rate constant to represent the effect of both processes.

Thus,

$$M = M_0 - M_0 e^{-Kt} + Ct \quad (7)$$

Where:

M = cumulative mass loss to current time t

$M_0 + Ct$ = linear long term mass loss

This equation was fitted to each set of results and thus for each sample the constant C represents the steady state loss and the constants M_0 and K show the extent and duration of the initial additional losses. These values are shown in Table 2 for the experimental results shown in Figure 5.

Table 2. Values of the constants of equation (7).
Results for mix C, Container 1, CC1.

Test age, days	Sample No.	C	Constants	
			M _o	K
3	1	0.026	1.186	0.056
3	2	0.024	1.240	0.055
28	1	0.019	0.784	0.067
28	2	0.019	0.689	0.061
90	1	0.016	0.545	0.131
90	2	0.015	0.547	0.155

Effect of sample thickness

A number of different coefficients have been used for vapour transmission rates. Henry and Kurtz (9) found the rate of transmission through concrete using the wet cup method (i.e. with water in the bottles as used in this work) to be independent of the sample thickness and used a coefficient which is independent of the thickness. Using the dry cup method (i.e. with dessicant in the bottles) Woodside (10), Wierig (11) and Spooner (12) assumed the rate to be proportional to thickness and Mills (13) derived a dependence on the square of the thickness.

The dependence on thickness in the data was checked by considering each similar pair of samples. For each pair the percentage difference in thickness and the percentage difference in the constants C, M and K were calculated. No correlation was found between any of the constants and the thickness and it was thus concluded that the rate is independent of thickness.

Effect of Relative Humidity (vapour pressure difference)

Henry and Kurtz (9) found some dependence on RH but only after 100 days. Wierig (11), however, reported a non-linear dependence.

In this paper dependence of the measured weight losses on relative humidity was investigated by plotting the relationship between the results from the samples exposed to different environments (Figure 6). It may be seen that there are clear linear relationships between the results from the different environments i.e. different relative humidities.

The target RH for container 1 was 70% and for container 2 it was 55.2% and thus a linear dependence of rate on RH would give a ratio of $(100-55.2)/100-70) = 1.49$. If Darcy's law is applied equation (6) shows that each of the terms is squared and this gives a ratio of 1.36. The other ratios are in Table 3.

Table 3. Effect of relative humidity on weight loss.

Container	Ratio of RH drop	Darcy Ratio	Observed C Ratio
2/1	1.49	1.36	0.95 (0.88)*
3/2	1.95	1.41	1.83 (0.85)*

*Figures in brackets after the ratios are the values of R squared for the relationship.

The data indicates that the losses from container 1 were higher than expected because of increased air circulation (container 1 was open but containers 2 and 3 were closed). The relationship between containers 2 and 3 shows a direct dependence on RH more than a Darcy relationship.

An average of the results for the three containers was obtained after multiplying the results from containers 1 and 3 by a constant factor to give each set the same mean value in order to give equal weighting. The average is plotted in Figure 7.

MEASUREMENT OF POROSITY

Two further sets of paste samples were cast and cured in the same way and were tested as follows:

One set was dried, ground, weighed and tested in a helium Autopycnometer to give the specific gravity. This machine measures the volume of helium that a sample displaces (i.e. the net volume). The sample is positioned in one of two chambers which initially have equal volumes. After evacuation an equal volume of helium is introduced into each chamber and the pressures are measured. The machine then calculated a volume change to the empty chamber to make the two volumes equal, i.e. to compensate for the presence of the sample. The volume change is effected with a piston and the helium is introduced again. The cycle repeats until equal pressures are found in both chambers at which time the volume of the sample is known from the position of the piston.

The second set was weighed wet and surface dry and then dried to constant weight at 110°C to give the dry density.

The porosity was then calculated from the specific gravity and the dry density. The results are presented in Figure 8. The consistent trends which may be observed in this figure indicate that the resolution of the measurements was adequate to differentiate the samples.

DISCUSSION

The mechanisms of transmission

The experiments indicate that the transmission of oxygen is adequately described by the Darcy equation, confirming findings of other workers (3,4,5). The mechanism of transmission of water vapour is clearly different. This difference is shown very clearly in

Figure 9 where the results of oxygen transmission are plotted against vapour transmission and the log of the oxygen permeability has similar range to the water transmission measurements. The observation that the water transmission rate is independent of the sample thickness severely limits the choice of possible mechanisms. The possibility of a continuously changing moisture content across the thickness consistent with a Darcy relationship is ruled out. Bazant and Najjar (14) observe that the mean free path of a molecule of water vapour at room temperature is many times greater than the size of continuous pores in concrete and Mills (13) observes that at 96% RH pores with diameters below 35 μm will sustain a meniscus. It may therefore be concluded that, with the exception of an outer surface layer, the pores are all either full of water or vapour at near 100% RH. Wierig (11) shows experimental readings of the vapour pressure across a wall with RH 95% and 0% on each side and it remains at 95% until the mid-point. He also shows a graph of transmission rate against thickness which indicates that the transmission rate is independent of thickness for thin samples, but dependent for thicker ones (more than 10 mm thick for mortar samples). The model proposed above would indicate that keeping one side at 100% RH would extend the range for which the transmission rate is independent of thickness.

Further support for the theory that this is not a vapour diffusion process is gained from the observation of water droplets on the underside of the samples. These droplets will clearly prevent the ingress of any gas or vapour into the sample. Rose (15) discussed the various degrees of saturation possible in a porous body. He suggests two mechanisms of transmission without full saturation, but without a vapour pressure gradient. One takes place when just the necks of the pores are filled with water, where vapour condenses on one side of the neck and evaporates from the other. The other mechanism is surface creep of a fine film of water coating the pore surfaces.

Powers (16) proposes a mechanism for the loss of water from the dry side. He observes that if it was necessary for water to evaporate from surfaces in the necks of the outer pores as in the “ink bottle” analogy virtually no water would be lost. He therefore proposes a mechanism where the process is controlled by the formation of vapour

bubbles in those pores at the surface which are of adequate size. The total areas which will be intersected by a cut through a sample will form the same fraction of the cut surface area as the fraction of the sample volume occupied by the pores, i.e. the porosity. This would indicate that the rate would be linearly dependent on porosity which may be seen to be a measure of a surface as well as bulk property. The relationship is shown in Figure 10 and it can be seen that the line is an excellent fit ($R^2 = 0.81$) but it does not pass through the origin (for the steady state 90 day porosity values were used). The data indicate that at porosity 11% the pores become either discontinuous or too small for bubble formation and the transmission stops.

The effect of test age

It may be seen from figures 7 and 8 that the vapour transport and porosity decrease with increasing maturity as expected. Figure 3, however, shows the oxygen permeability increasing with time for the SF samples from curing condition 1 (moist cure at 20°C). It is possible that this could have been caused by open porosity caused by the depletion of lime during the progress of the pozzolanic reaction but the absence of this effect in the dry cure samples (CC2) indicates that it was caused by cracking as a result of the drying procedure on the SF samples. It is therefore indicated that the conditions most likely to produce samples which are virtually impermeable to oxygen in normal environments are prolonged moist curing of SF samples with low w/c ratios.

The relative importance of the two measurements

The results from the vapour transmission experiment have been presented in units of weight loss because of the permeability model used for the oxygen results was not correct for the physical process. If the equations are used, however, to obtain an estimate of the relative effect of the two processes the permeability coefficients in m^2 are equal to 7×10^{-16} times the weight loss in g/100 day. This calculation assumes that the transmission of water is by pure vapour permeation and should therefore be treated with considerable caution, a value of 10^{-5} has been used for the viscosity of water vapour. Using this factor

the measured water permeabilities lie in the range of 2×10^{-15} to 21×10^{-16} while the oxygen permeabilities lie in the range of 10^{-15} to 10^{-21} . These results imply that the transport rates of water and oxygen in the control mixes are similar but the use of the SF with a low water cement ratio (mix A) could cause the permeability to oxygen to become significantly lower than that for water. The major increase in the sensitivity to different curing regimes shown in Figure 3 is, however, a cause for concern if this property is to be used. In particular the increase in permeability with curing time for both SF mixes in Curing Condition 1 (20°C) is of interest.

The observed sensitivity of the water vapour transport rates to the different curing conditions will have been reduced by the effect of continuing hydration during the experiments.

The effect of water vapour on the oxygen permeability

All of the samples tested for oxygen permeability in this work were dried before testing. Measuring gas permeabilities at other humidities is difficult because both the samples and the gas to be permeated through them must be equilibrated to the required humidity at the start of the test and the entire system must be sealed from the atmosphere during the test to prevent drying. Preliminary results from experiments of this type have been reported (Atkinson et. al. (17)) and show the permeability of a grout falling from 3×10^{-16} when dry to 3×10^{-18} at 75% RH and to below 10^{-21} at close to 100% RH. If a similar effect was observed with samples of mix A where the permeability is already low the effect would create an almost impermeable barrier to oxygen.

The effect of the corrosion rate

Inhibition of corrosion due to lack of oxygen is only usually observed in structures submerged in a substantial depth of water. In the laboratory it is very difficult to observe because the oxygen included in the original mix is sufficient to sustain corrosion for experimental timescales. It is possible, however, that SF concretes could be sufficiently

impermeable to control corrosion in this way. The effect of the SF on water vapour transport is substantially less significant and therefore unlikely to reduce corrosion.

CONCLUSIONS

1. Transport of oxygen through dry cementitious samples is accurately described by the Darcy equation and the measured permeabilities vary over a substantial range of values.
2. The rate of transport of water vapour was not found to vary greatly for the different samples and was proportional to the porosities of the samples.
3. The results indicate that under the correct conditions SF could be used to make a material which is almost impermeable to oxygen.

REFERENCES

1. Gjorv O E
Durability of concrete containing condensed silica fume.
ACI publication SP-79. Proceedings of the first international conference on the use of fly ash, silica fume, slag and other mineral by-products in concrete. Canada 1983, pp.695-708.
2. British Standards Institute.
British standard 882, 1201. Part 2. 1973. Aggregates from natural sources for concrete. BSI London.
3. Cabrera J G and Lynsdale C J
A simple gas permeameter for the measurement of concrete permeability.
Magazine of Concrete Research, Vol. 40, No. 144, September 1981.
4. Lawrence C D.
Durability of concrete: molecular transport processes and test methods. Cement and Concrete Association, Technical Report 544, 1981.
5. Lawrence C D.
Measurements of permeability. Proc. 8th Int. Congress on the Chemistry of Cement, Rio de Janeiro 1986. FINEP, 1986, Vol V. pp. 29-34.
6. Bamforth P B.
The relationship between permeability coefficients for concrete obtained using liquid and gas. Magazine of Concrete Research, Vol. 9, 1987, pp. 3-11.
7. Nagataki S and Ujike I.
Air permeability of concretes mixes with fly ash and silica fume ACI publication SP91, Proceedings of the 2nd Int. CANMET/ACI Conference on the Use of Fly

- Ash, Silica Fume, Slag and Natural Pozzolans in Concrete. Madrid, 1986, pp. 1049-1068.
8. Sneek T and Oinonen H.
Measurements of pore size distribution of porous materials. The State Institute for Technical Research, Finland, unpublished report, 1970.
 9. Henry R L and Kurtz G K.
Water vapour transmission of concrete and of aggregates. U S Naval Civil Engineering Laboratory, Pot Hueneme, California, June 1963.
 10. Woodside W.
Water vapour permeability of porous media. Canadian Journal of Physics 37, No. 4, 1959, pp 413-416.
 11. Wierig H-J.
Die Wasserdampfdurchlässigkeit von Zementmortel und Beton. Zement-Kalk-Gips 18, No. 9, Sept 1965, pp. 471-482.
 12. Spooner D C.
The practical relevance of mechanisms of water and water vapour transport in porous building materials. Autoclaved Aerated Concrete, Moisture and Properties, ed. Wittman F H. Elsevier Scientific Publishing, 1983, pp. 27-41.
 13. Mills R H.
Mass transfer of water vapour through concrete. Cement and Concrete Research, Vol. 15, 1985, pp.74-82.
 14. Bazant Z P and Najjar L J.

- Non-linear water diffusion in non-saturated concrete. *Materiaux et Constructions* Vol. 5, No. 25, 1972, pp. 1-8.
15. Rose D A.
Water movement in unsaturated porous material. *Rilem Bulletin*, No. 29, Dec. 1965, pp. 119-124.
 16. Powers T C.
Physical properties of cement paste and concrete. Washington D C, 1960, pp. 577-613.
 17. Atkinson A, Claisse P A, Harris A W and Nickerson A K.
Mass transfer in water saturated concretes. *Material Research Society Symposium Proceedings. Scientific Basis for Nuclear Waste Management XIV*, Boston, pp. 741-749. Vol 176 1990..



Figure 1. Leeds Gas Permeameter.

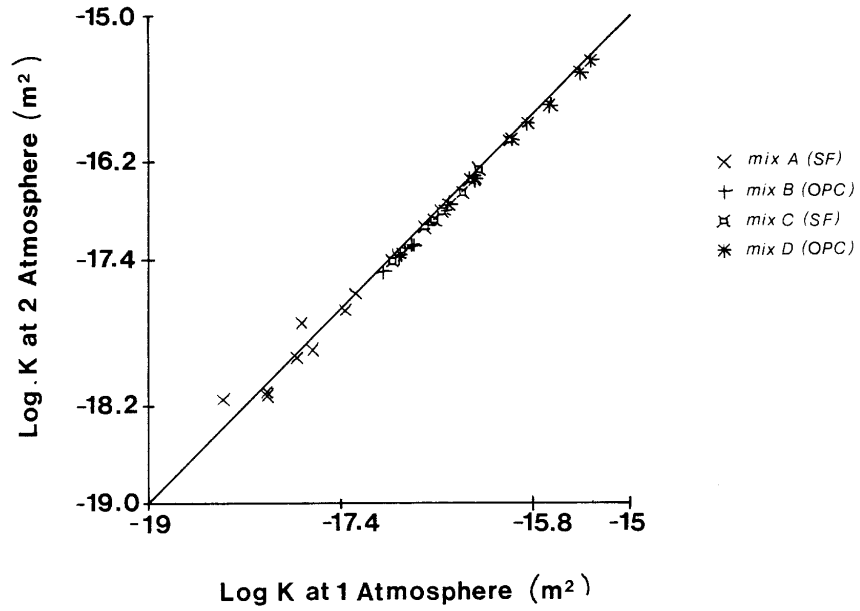


Figure 2. Relationship between measurements of the oxygen permeability K made at 1 atmosphere pressure drop and those at 2 atmospheres. The line drawn is that of equality ($Y=X$).

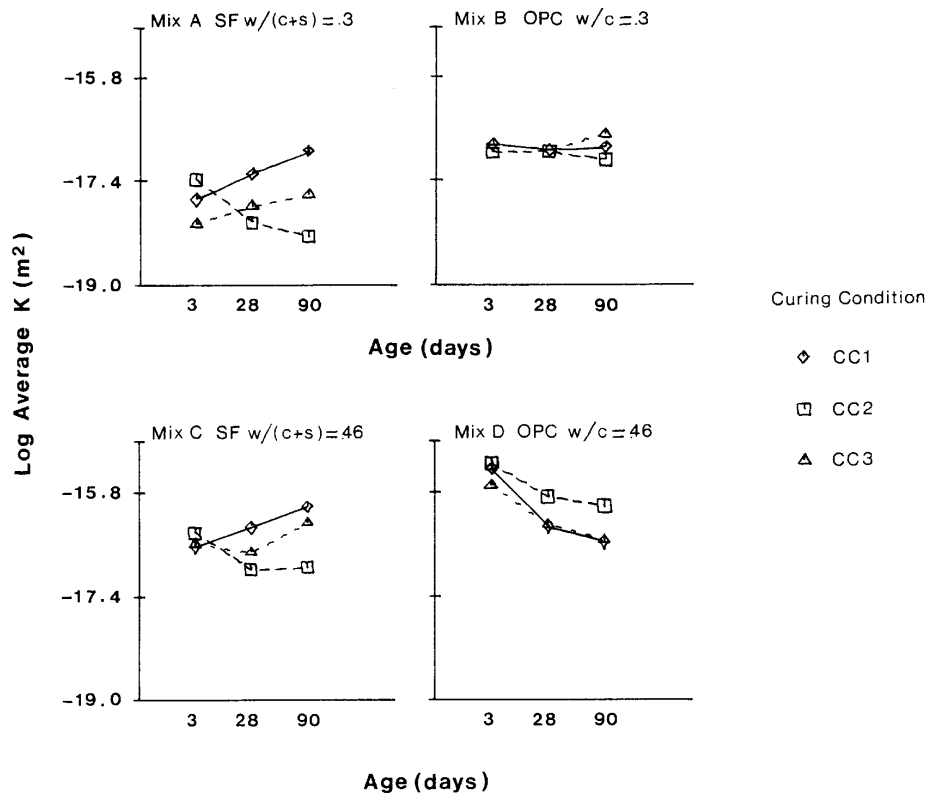


Figure 3. Oxygen permeability K calculated from an average of the readings at 1 and 2 atmospheres.

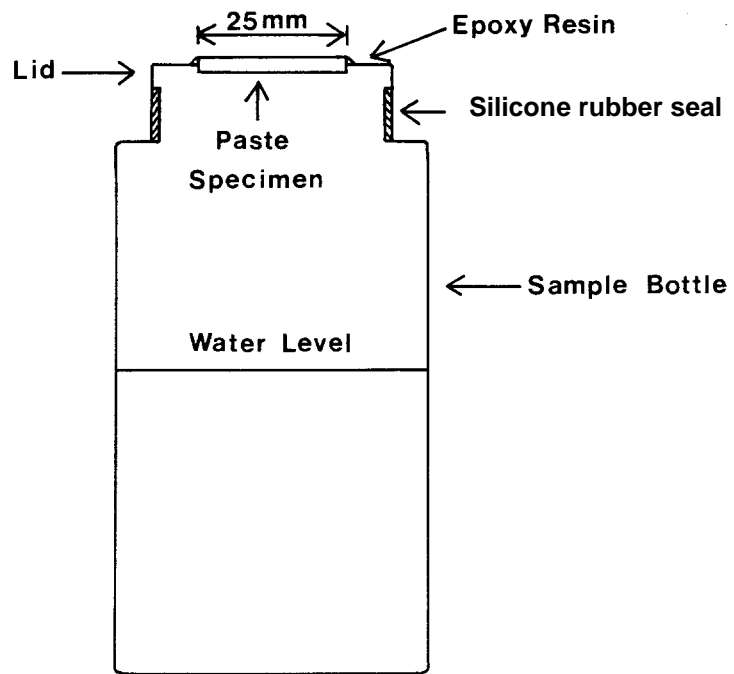


Figure 4a. Detail of bottle for vapour transmission measurement.

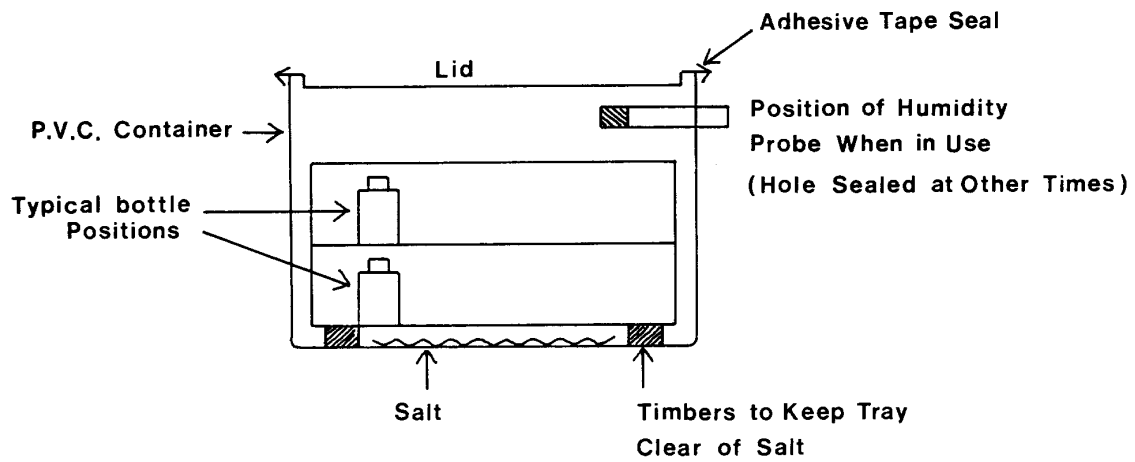


Figure 4b. Details of container.

Container 1: Open to the atmosphere in a room controlled at 70% RH

Container 2: Sealed with a quantity of sodium dichromate in the bottom to give an RH of 55.2% (Sneck and Oinonen (7)).

Container 3: Sealed with a quantity of lithium chloride to give an RH of 12.4%.

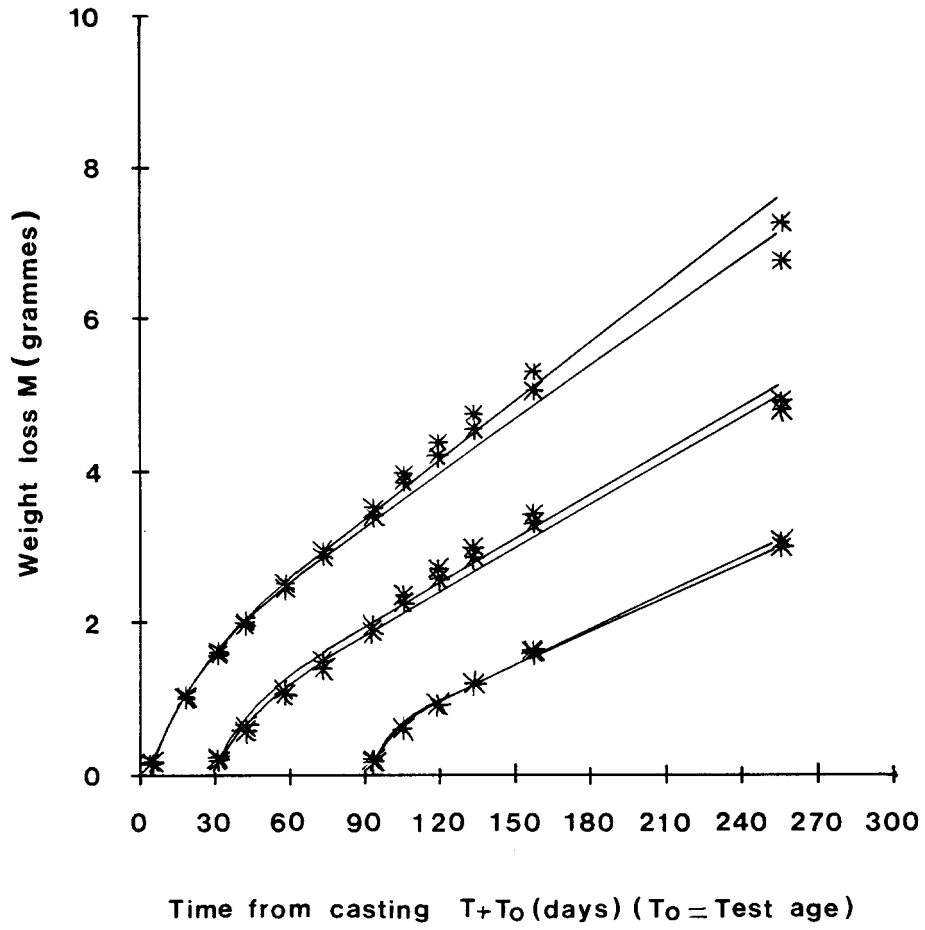


Figure 5. Typical outputs for vapour transmission Mix C, Container 1, CC1

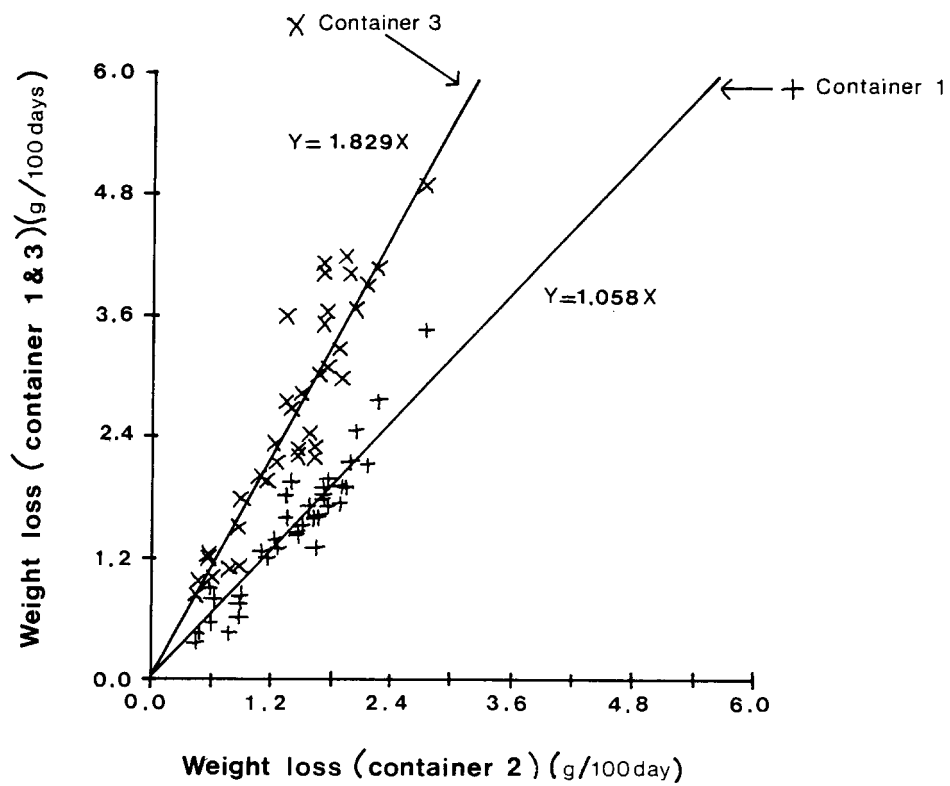


Figure 6. Relationship between the weight losses of equivalent samples in the different containers.

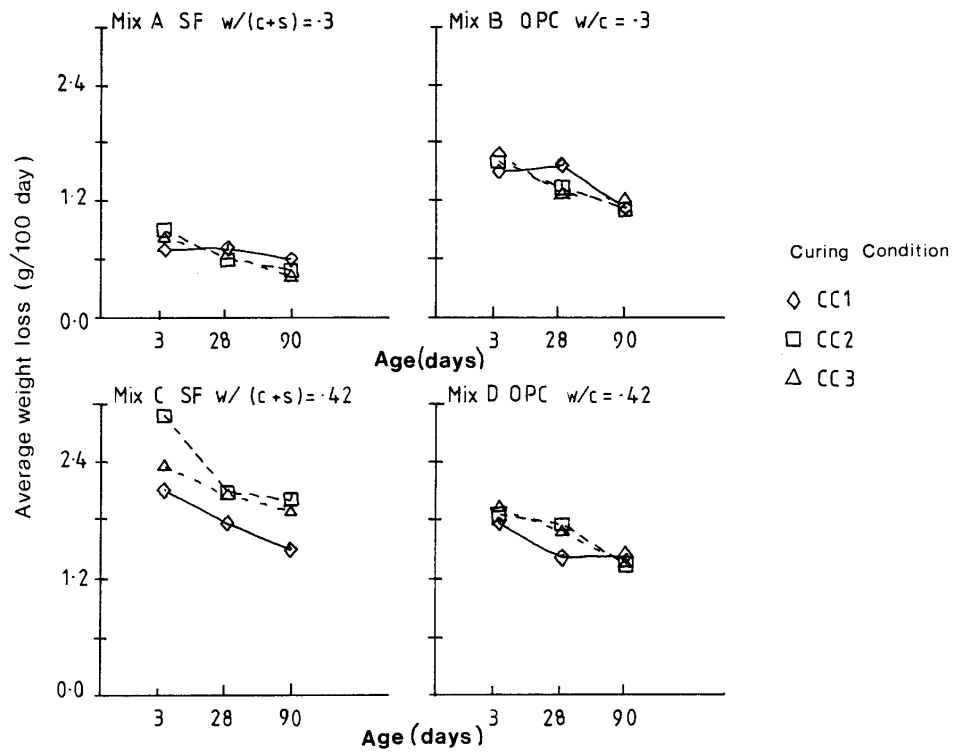


Figure 7. Average weight loss from the three containers (all normalised to the same average as container 2).

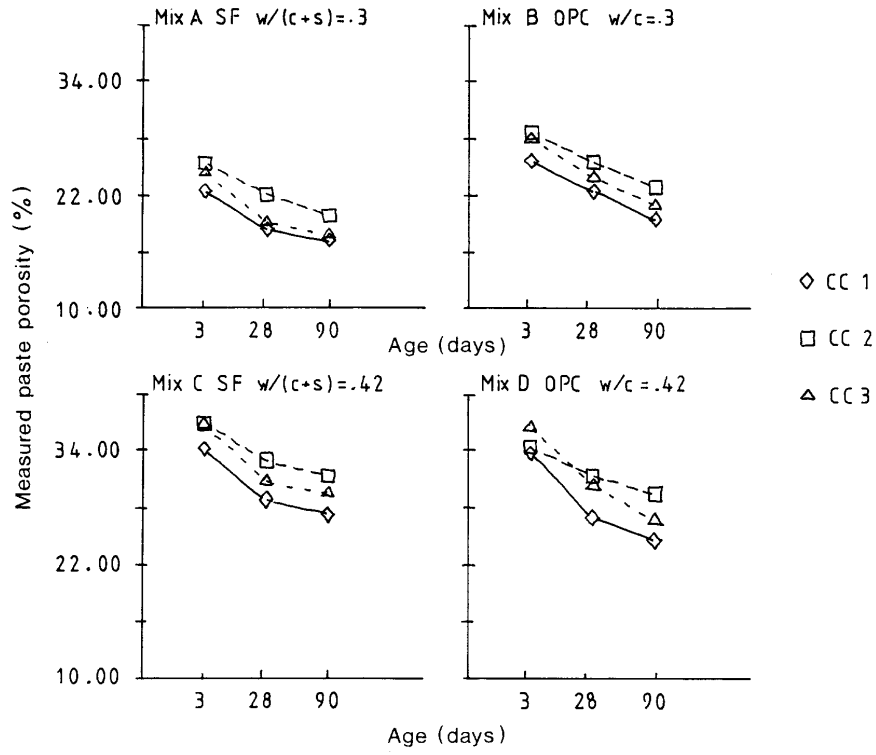


Figure 8. Porosity results for paste samples (obtained by helium intrusion).

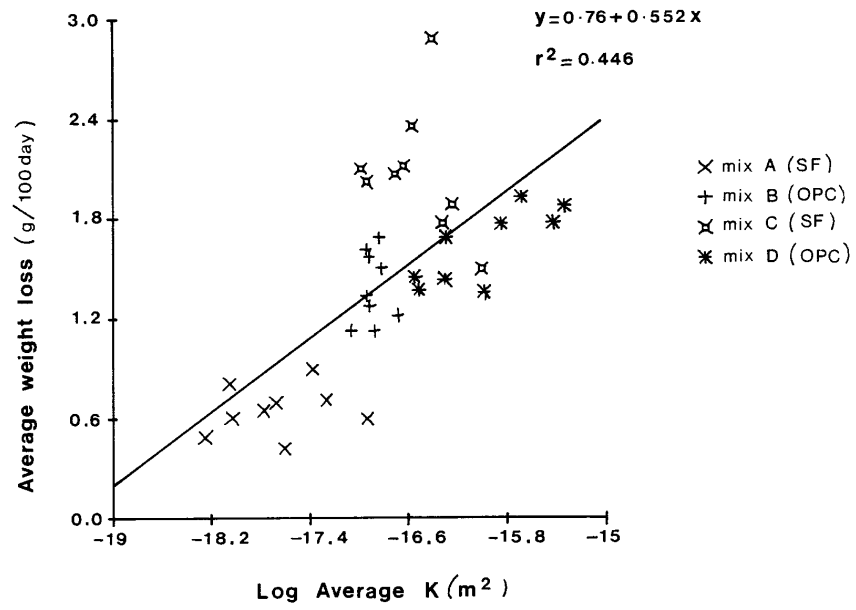


Figure 9. Relationship between the permeabilities to oxygen and water.